

11

Gas–Liquid-phase Reactions: Miscellaneous Reactions

Ilhyong Ryu and Md Taifur Rahman

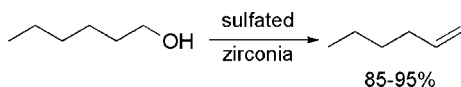
11.1

Dehydration

The dehydration of 1-hexanol to 1-hexene, using a sulfated zirconia catalyst (zirconia treated with sulfuric acid) [1, 2], can be performed in a microflow reactor [3]. 1-Hexanol is pumped through the reactor chip at a flow rate of $3 \mu\text{L min}^{-1}$ at 155°C . The conversion of 1-hexanol to 1-hexene is on average between 85 and 95% (Scheme 11.1). This conversion efficiency is extremely good compared with the 30% yield expected for the industrial process. The reaction can also be applied to ethanol. Only trace amounts of ethanol are detected, with most of the feedstock being converted to ethylene (68%), ethane (16%) and methane (15%).

Rouge *et al.* examined the dehydration of 2-propanol to propene using a microreactor [4]. The microreactor consisted of stacked plates, each containing 34 rectangular channels of $300 \mu\text{m}$ width, $240 \mu\text{m}$ depth and 20 mm length. The catalyst, $\gamma\text{-Al}_2\text{O}_3$, was deposited as layers in the microchannels. Periodic concentration cycling was performed by switching between the feed flow of 2-propanol and an inert gas (nitrogen) flow. Based on the kinetic model developed with the fixed-bed reactor, the dynamic behavior of the microreactor under periodic concentration variation was simulated (Figure 11.1). On switching from alcohol feed to inert gas in a cycle period of 30 s, a sharp peak corresponding to the product, propene, appeared due to the so-called stop effect.

Recently, Chen and coworkers reported on catalytic dehydration of bioethanol to ethylene over $\gamma\text{-Al}_2\text{O}_3$ doped with TiO_2 using a stainless-steel microreactor [5]. In the microreactor, 30 microchannels of $1000 \mu\text{m}$ width, $1250 \mu\text{m}$ depth and 3 cm length per chip are separated by $500 \mu\text{m}$ fins. Catalyst particles of size 40–60 mesh are packed within the 30 parallel channels. Quartz wool is set at each end of the catalysts to keep them from moving with the stream flow. The channels are sealed with graphite sheet covers. Alumina catalysts doped with 10 wt.% titanium oxide gave excellent results in terms of high ethanol conversion, ethylene selectivity to diethyl ether and yields. For example, the conversion of ethanol was 99.7% at a liquid hourly



Scheme 11.1 Dehydration of 1-hexanol to 1-hexene, using a sulfated zirconia catalyst.

space velocity of 52 h^{-1} at 440°C , corresponding to a yield of ethylene of $26 \text{ g}_{\text{cat}}^{-1} \text{ h}^{-1}$ with 98.6% selectivity. The yield of ethylene in the microreaction system was two orders of magnitude higher than that in the traditional fixed bed reactor.

Although it is not a gas-phase but a solution-phase reaction, Fukase and coworkers employed microflow systems for the acid-catalyzed dehydration of allylic alcohols to give dienes. The microfluidic dehydration effectively took place at 80°C using *p*-TsOH as a catalyst and THF and toluene as solvents. Both an IMM standard micromixer and a PTFE (Teflon) Comet X01 reactor performed the dehydration successfully [6].

11.2

Phosgene Synthesis

Phosgene (COCl_2) is a very important intermediate in the polymer and pharmaceutical industries. The reaction of CO with Cl_2 to give phosgene is moderately fast and exothermic ($-26 \text{ kcal mol}^{-1}$). Because of the highly toxic and hazardous nature of both the starting materials and product, phosgene production requires strict safety measures.

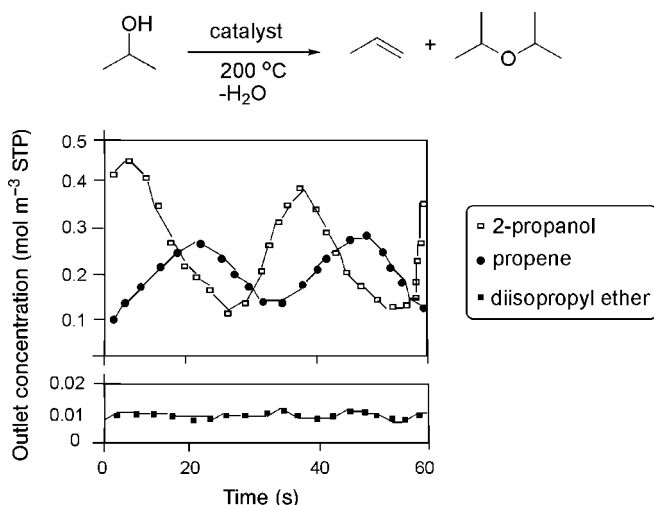


Figure 11.1 Dehydration of 2-propanol.

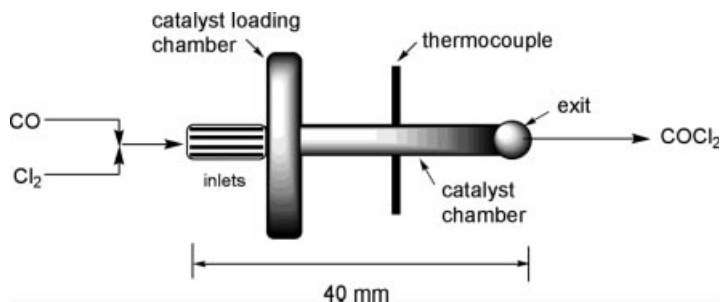


Figure 11.2 Microflow system for the synthesis of phosgene.

Jensen and coworkers studied phosgene synthesis using a micropacked-bed reactor [7]. A silicon reactor consisting of a 20 mm long, 625 μm wide and 300 μm deep reaction channel (volume 3.75 mL) was employed (Figure 11.2). In order to avoid corrosion by chlorine, the microchannels were coated with a thin silicon dioxide film (5000 \AA). A fixed bed of activated carbon catalyst (1.3 mg, 53–73 μm) supported on alumina particles (~ 3 mg, 53–71 μm) was placed inside the microchannel. Chlorine and CO were mixed and fed into the microchannel network. The exit stream could be analyzed on-line using a mass spectrometer.

At a 4.5 std. $\text{cm}^3 \text{min}^{-1}$ total feed rate with a Cl_2 :CO ratio of 1:2, conversion of chlorine to phosgene increased with increase in temperature and attained a maximum value at 200 $^\circ\text{C}$ (Figure 11.3). Due to the high heat-dissipating capacity of the silicon microreactor, no hot-spot was formed, which is evidenced from the total avoidance of any other side-products in this process. With this single device, the projected phosgene production is 3.5 kg per year. They also demonstrated on-site use of phosgene to prepare isocyanate by reaction with cyclohexylamine.

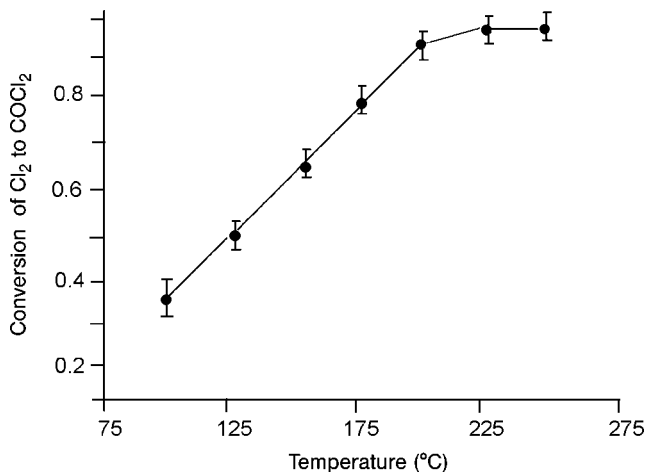


Figure 11.3 Temperature effect on the synthesis of phosgene.

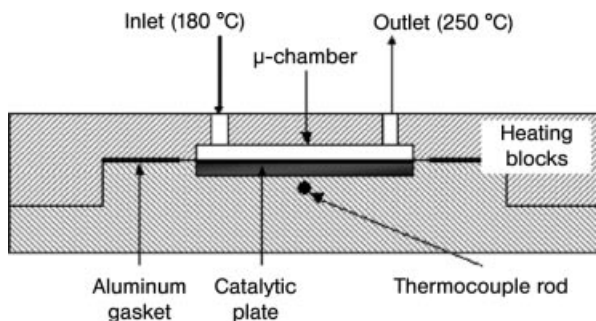


Figure 11.4 Microchamber test reactor for AISI316L plate-supported catalysts.

11.3

Fischer–Tropsch Synthesis

The Fischer–Tropsch synthesis is used to synthesize hydrocarbons from CO and H₂. Guillou *et al.* reported Fischer–Tropsch synthesis using a microreactor made by stacking a single catalytic plate between two mechanically engineered AISI316L blocks (40 × 20 × 250 mm channel) (Figure 11.4) [8]. The catalyst was 20 wt.% Co/SiO₂ grafted on a stainless-steel substrate.

Using this microreactor, the influence of composition (H₂:CO ratio) was investigated with a 1 s residence time. A higher relative H₂ partial pressure resulted in a higher conversion of CO (H₂:CO = 1.5, 10% conversion; H₂:CO = 3, 16% conversion). Moreover, higher H₂ caused a progressive shift of the distribution towards shorter hydrocarbons (Figure 11.5).

The influence of reaction temperature was also tested. Reaction at 220 °C resulted in higher CO conversion (24.1%). The product distribution was sensitive to temperature: higher temperatures induced a shift towards the production of shorter hydrocarbons (Figure 11.6). Light hydrocarbons were mainly formed at 220 °C. The productivity was higher under microchamber conditions than in a classical fixed-bed

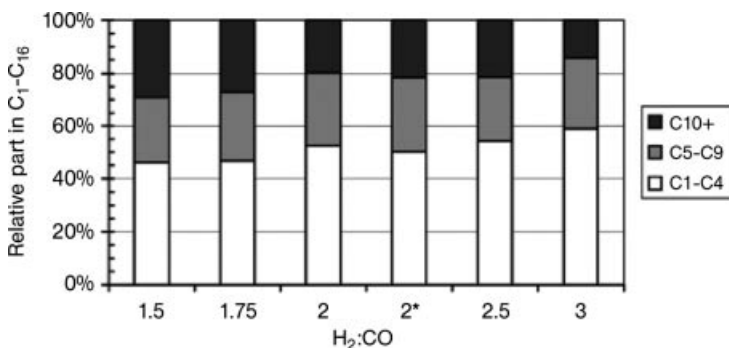


Figure 11.5 Product distribution (H₂:CO = 1.5–3, at 180 °C, 50 μm thick catalyst).

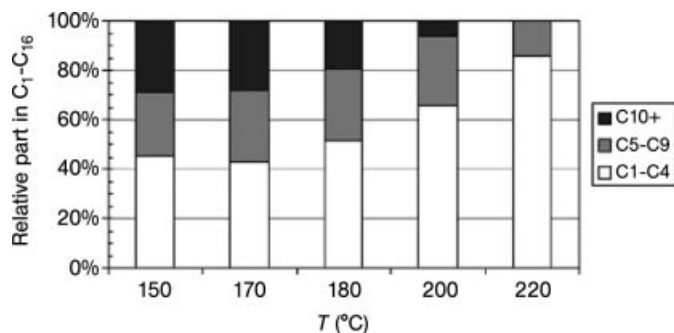


Figure 11.6 Products distribution (150–220 °C, $H_2/CO = 2$, 70 μm thick catalyst).

reactor [microchamber, $660 \text{ mol(CO) g(catalyst)}^{-1} \text{ s}^{-1}$; fixed-bed reactor, $27 \text{ mol(CO) g(catalyst)}^{-1} \text{ s}^{-1}$]. This was attributed to the increase in mass and heat transfer within the microdevice.

Dagle *et al.* reported CO methanation with hydrogen using a microreactor [9]. Selective CO methanation as a strategy for CO removal in fuel processing applications was investigated over an Ru-based catalyst. A 3% Ru/ Al_2O_3 catalyst with a 34.2 nm crystallite was shown to be capable of reducing CO in a reformat to less than 100 ppm over a wide temperature range from 240 to 280 °C, while keeping hydrogen consumption below 10%.

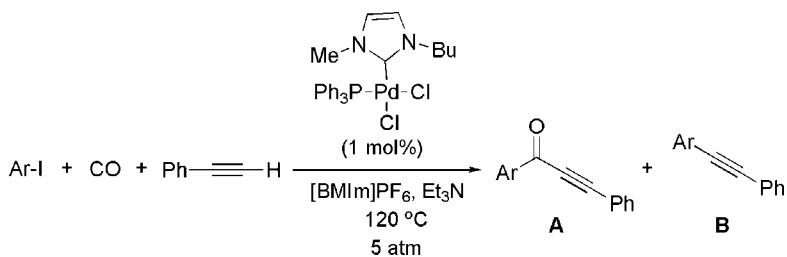
11.4 Carbonylation

Carbonylation using CO gas is a fundamentally important reaction for incorporating carbonyl functionality into organic molecules. Recently, several groups have reported on the utilization of microreaction devices for effective carbonylation reactions.

Ryu's group developed a low-pressure microflow system for palladium-catalyzed multiphase carbonylation reactions using an ionic liquid as a reaction medium. This microflow system consists of T-shaped micromixer (i.d. 400/1000 μm) and a tubular residence time unit (i.d. 1000 μm) that is capable of working under various CO pressures and temperatures. Pd-catalyzed carbonylative Sonogashira coupling of an aryl iodide and phenylacetylene in the presence of CO in an ionic liquid, [BMIm]PF₆, gave an α,β -acetylenic ketone as sole product in high yield when this microflow system was used (Table 11.1) [10]. Interestingly, when a batch reactor, i.e. an autoclave, was employed for the same reaction, Sonogashira coupling byproduct dominated over α,β -acetylenic ketone [11]. This tendency generally holds also for other substrates.

For the Pd-catalyzed amidocarbonylation reaction between iodobenzene and Et_2NH at a CO pressure of 20 atm, this microflow system produced an α -ketoamide in 80% yield along with 6% of amide, whereas a batch reaction suffered from a lower yield of the α -ketoamide (63%) (Table 11.2). The authors found that a multiphase

Table 11.1 Pd-catalyzed carbonylative three-component coupling reaction.



Ar-I	System	Yield (%)	
		A	B
	Microflow	83	–
	Batch	25	60
	Microflow	77	–
	Batch	67	21
	Microflow	92	–
	Batch	36	37
	Microflow	72	–
	Batch	65	16

(gas-liquid) segmented flow pattern occurred inside the microtube, which possibly contributed to better carbonylation selectivity in the microflow system compared with the conventional macrobatch reactors.

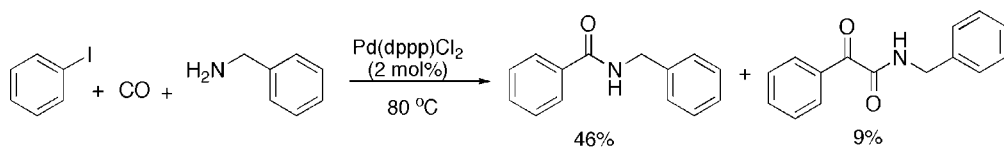
The synthesis of amides based on carbonylation was also reported by de Mello and coworkers (Scheme 11.2) [12]. They employed a glass microreactor with channel dimensions of 200 μm (wide) \times 75 μm (deep) \times 5 m (long), in which they investigated the effect of reactant flow rate, under a constant stream of CO. Using the synthesis of *N*-benzylbenzamide as a model reaction, they found that employing a biphasic reaction setup, comprising gaseous CO and a solution of iodobenzene, benzylamine and a Pd-phosphine catalyst, annular flow dominated (whereby liquid is forced to the surface of the microchannel and gas flows through the center) when flow rates in the range 5.0–20.0 $\mu\text{L min}^{-1}$ were employed. Conducting microreactions for 10 min and analyzing the reaction products by gas chromatography, the authors reported an increase in conversion as a function of residence time, which they attributed to the formation of a stable flow regime within the reactor. Using the optimal flow rate of 5.0 $\mu\text{L min}^{-1}$, 46% of amide was obtained, along with 9% of α -ketoamide; in contrast, a comparable batch reaction afforded only 25% amide and no α -ketoamide.

Table 11.2 Pd-catalyzed single/double carbonylation of aryl iodides.

Ar-I	System	Yield (%)	
		A	B
	Microflow	6	80
	Batch	11	63
	Microflow	5	85
	Batch	4	70

Jensen and coworkers employed a silicon microreactor (Figure 11.7) to perform aminocarbonylation reactions of aryl halides with morpholine [13]. The results show that carbonylation selectivity (mono- versus double carbonylation) depended on the reaction temperatures and CO pressures (Table 11.3). They also demonstrated that high-throughput screening of the optimal reaction conditions (temperature and pressure) could be performed with their system.

de Mellow and coworkers reported solid-liquid-gas carbonylation reactions employing a silica-supported palladium catalyst into a PTFE (Teflon) tube (Figure 11.8) [14]. They carried out aminocarbonylation of aryl halides and benzylamine in the presence of [^{11}C]carbon monoxide to obtain ^{11}C -labeled amides for applications in positron emission tomography (PET). Their microreaction system showed superior performance (amide yields 26–99%) to the batch reactor (amide yields <50%). They also demonstrated the on-line production of [^{11}C]carbon monoxide and its subsequent use in the microflow aminocarbonylation.

**Scheme 11.2** Synthesis of *N*-benzylbenzamide via a gas-liquid carbonylative cross-coupling reaction.

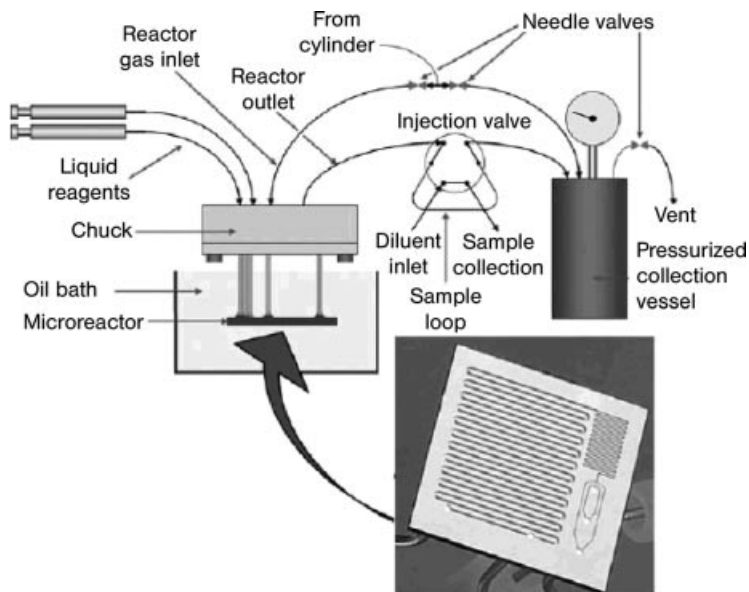
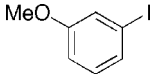
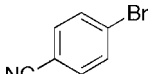
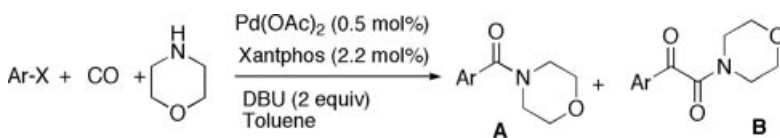


Figure 11.7 Microreactor setup for aminocarbonylation.

Carbonylation using microreactors is not necessarily restricted to metal-catalyzed systems. Ryu and coworkers found that radical reactions proceeded more rapidly in a microreactor than in a batch reactor [15]. They also investigated radical carbonylation using a continuous microflow reactor system consisting of a MiChS micromixer

Table 11.3 Aminocarbonylation reactions of aryl halides with morpholine.

				Yield (%)	
Ar-X	Pressure (bar)	Temperature (°C)	Time (min)	A	B
	7.9	146	3.3	68	28
		116	4.2	35	65
	2.7	160	7.1	83	0
		14.8	109	6.6	32



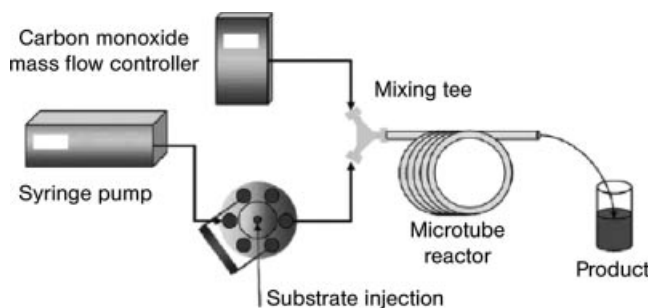


Figure 11.8 Microreactor for radiolabeling with ^{11}C .

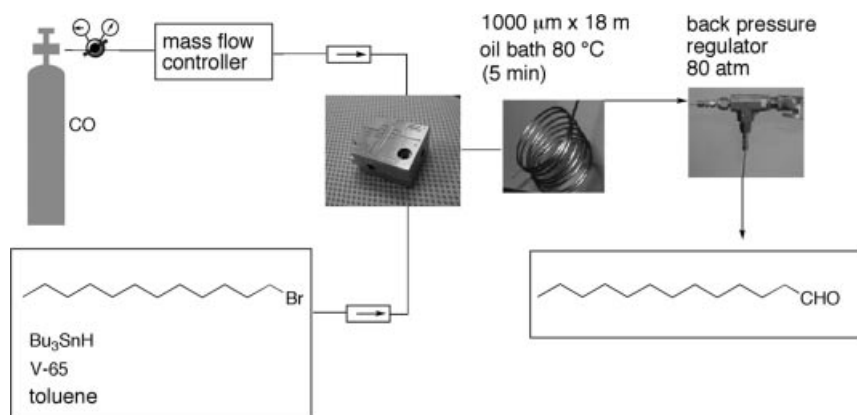


Figure 11.9 Radical carbonylation in a microflow system.

(www.michs.jp). When a toluene solution of 1-bromododecane and tributyltin hydride and V-65 (10 mol%) was mixed with CO in a MiChS micromixer and passed through a tubular residence time unit at $80\text{ }^{\circ}\text{C}$ with a residence time of 5 min, the reaction was complete and the undecanal product was obtained in good yield (Figure 11.9) [16]. The slow decomposition time of AIBN prevented the achievement of such a short reaction time and changing the radical initiator to V-65, which decompose more rapidly than AIBN, was fruitful.

11.5 Conclusion

Advantageous features of microreaction devices, such as high surface area-to-volume ratio and efficient heat-transfer, were exploited by several research groups to conduct a number of gas-liquid synthetic reactions. In many cases, microreaction provided higher yields and better selectivity when compared to conventional batch

reactors. Moreover, reactions that require forcing conditions (e.g. high temperature) or use of poisonous gases could be conducted safely with the miniaturized chemical reactors.

References

- 1 M. Nitta, H. Sakoh, K. Aomura, *Appl. Catal.* **1984**, *10*, 215–217.
- 2 D. Das, D. K. Chakrabarty, *Energy Fuels* **1998**, *12*, 109–114.
- 3 N. G. Wilson, T. McCreedy, *Chem. Commun.*, **2000**, 733–734.
- 4 A. Rouge, B. Spoetzl, K. Gebauer, R. Schenk, A. Renken, *Chem. Eng. Sci.* **2001**, *56*, 1419.
- 5 G. Chen, S. Li, F. Jiao, Q. Yuan, *Catal. Today* **2007**, *125*, 111–119.
- 6 K. Tanaka, S. Motomatsu, K. Koyama, S. Tanaka, K. Fukase, *Org. Lett.* **2007**, *9*, 299–302.
- 7 S. K. Ajmera, M. W. Losey, K. F. Jensen, M. A. Schmidt, *AIChE J.* **2001**, *47*, 1639.
- 8 L. Guillou, D. Balloy, P. Supiot, V. Le Courtois, *Appl. Catal. A* **2007**, *324*, 42.
- 9 R. A. Dagle, Y. Wang, G.-G. Xia, J. J. Strohm, J. Holladay, D. R. Palo, *Appl. Catal. A* **2007**, *326*, 213.
- 10 M. T. Rahman, T. Fukuyama, N. Kamata, M. Sato, I. Ryu, *Chem. Commun.* **2006**, 2236–2238.
- 11 T. Fukuyama, R. Yamaura, I. Ryu, *Can. J. Chem.* **2005**, *83*, 711–715.
- 12 P. W. Miller, N. J. Long, A. J. de Mello, R. Vilar, J. Passchier, A. Gee, *Chem. Commun.* **2006**, 546–545.
- 13 E. R. Murphy, J. R. Martinelli, N. Zaborenko, S. L. Buchwald, K. F. Jensen, *Angew. Chem. Int. Ed.* **2007**, *46*, 1734.
- 14 P. W. Miller, N. J. Long, A. J. de Mello, R. Vilar, H. Audain, D. Bender, J. Passchier, A. Gee, *Angew. Chem. Int. Ed.* **2007**, *46*, 2875.
- 15 T. Fukuyama, M. Kobayashi, M. T. Rahman, N. Kamata, I. Ryu, *Org. Lett.* **2008**, *10*, 583.
- 16 T. Fukuyama, M. T. Rahman, N. Kamata, I. Ryu, to be published.